Materials Today Communications 33 (2022) 104674

Contents lists available at ScienceDirect

Materials Today Communications

journal homepage: www.elsevier.com/locate/mtcomm

Development and characterisation of strontium-doped sol-gel coatings to optimise the initial bone regeneration processes

I. García-Arnáez [a,*], A. Cerqueira [b], F. Romero-Gavilán [b], F. Elortza [c], M. Azkargorta [c], I. Iloro [c], J. Suay [b], I. Goñi [a], M. Gurruchaga [a]

[a] Departament of Polymers and Advanced Materials: Physics, Chemistry and Technology, University of the Basque Country (UPV/EHU), P. M. de Lardizábal, 3, 20018 San Sebastián, Spain

[b] Department of Industrial Systems Engineering and Design, Universitat Jaume I, Av. Vicent Sos Baynat s/n, 12071 Castellón de la Plana, Spain

[c] Proteomics Platform, CIC bioGUNE, Basque Research and Technology Alliance (BRTA), CIBERehd, ProteoRed-ISCIII, Bizkaia Science and Technology Park, 48160 Derio, Spain

ARTICLE INFO

Keywords:
Dental implants
Proteomics
Osteogenesis
Biomedical applications
Bone regeneration

ABSTRACT

Strontium plays an important role in bone regeneration; it promotes the differentiation and maturation of osteoblasts and inhibits the activity of osteoclasts. Our principal objective in this study was to formulate new organic-inorganic hybrid sol-gel coatings applied to titanium discs. These coatings were functionalised with different amounts of $SrCl_2$ and examined using *in vitro* tests and proteomics. The chemical and morphological characteristics of obtained coatings were scrutinised. The *in vitro* evaluation using the MC3T3-E1 osteoblasts and RAW264.7 macrophages showed the osteogenic and anti-inflammatory effects of strontium doping. The proteomic assay identified 111 different proteins adhering to the coatings. Six of these proteins reduced their adhesion affinity as a result of Sr-doping, whereas 40 showed increased affinity. Moreover, the proteomic analysis revealed osteogenic and anti-inflammatory properties of these biomaterials. The analysis also showed increased adhesion of proteins related to the coagulation system. We can conclude that proteomic methods are invaluable in developing new biomaterials and represent an important tool for predicting the biocompatibility of dental implants.

1. Introduction

Strontium (Sr) is a trace element found in the bone (0.00044% of body mass), with close similarities to calcium (Ca) owing to its bone-seeking properties [1]. It is involved in bone formation; it promotes the proliferation and osteogenic differentiation of osteoblasts [2,3] and inhibits the activity of osteoclasts responsible for bone resorption [4]. It can also reduce the production of matrix metalloproteinases and induce osteoclast apoptosis via calcium-sensing receptor dependent mechanism [5]. Moreover, Sr can enhance the replication of pre-osteoblastic cells by activating the ERK-MAPK and Wnt signalling [6]. Small amounts of this element can stabilise the bone structure, positively affecting osteogenesis [7]. Strontium has attracted the attention of several research groups due to its effect on the regeneration of bone tissue. As a result, new biomaterials releasing Sr [8] have been designed and studied. The silica sol-gel hybrid networks have been already used to develop biomaterials with osteogenic behaviour [9]. Almeida et al. have synthesised a hybrid material based on the PDMS-SiO_2 system with the capacity to release Sr for the induction of bone tissue repair [10]. Moreover, Omar et al. have obtained sol-gel coatings using Sr-functionalised silica nanoparticles, achieving an *in vivo* improvement in bone morphology and quality [11]. Likewise, John et al. have developed hybrid Sr-scaffolds showing promising *in vitro* results [12].

Strontium is increasingly used in clinical bone regeneration and treatments for bone diseases such as osteoporosis [13,14]. For example, strontium ranelate and chloride have been used in osteoporosis to reduce the risk of bone fractures [15]. In dental applications, Sr improves and shortens the recovery after implantation. Zhang et al. described a titanium implant with a nanoporous Sr-surface achieving fast osseointegration, improving angiogenesis and osteogenesis [16].

However, the effects of different Sr concentrations should be taken into account. A low dose of Sr promotes osteogenesis, although some

* Correspondence to: Departamento de Polímeros y Materiales Avanzados: Física, Química y Tecnología, Laboratorio de Biomateriales Poliméricos, Campus de Gipuzkoa, Paseo Manuel de Lardizabal 3, 20018 Donostia, Spain.

E-mail address: inaki.garciaa@ehu.eus (I. García-Arnáez).

https://doi.org/10.1016/j.mtcomm.2022.104674
Received 16 March 2022; Received in revised form 8 September 2022; Accepted 10 October 2022
Available online 13 October 2022

studies report slight toxicity [17]. Neves et al. have stated that small amounts of Sr positively impact the bone formation and remodelling [8]. Likewise, Schrooten et al. report that the effect of Sr on bone formation and mineralisation is dose-dependent [18].

Immediately after implantation, interactions between the biomaterial and blood [19,20] result in the adsorption of proteins on the surface of the implant through a competitive displacement mechanism known as the Vroman effect [21]. The type, conformation and quantity of these proteins depend on the surface characteristics of the biomaterial. Therefore, the chemical properties of the surface, its wettability and roughness, among others, will determine the composition of the protein layer adsorbed to the biomaterial [22].

Cells interact with this layer of proteins [23]; they respond to the adsorbed proteins and not to the surface of the material [24]. The success of osseointegration of the implant and the regeneration of the bone relies on various processes of immune response, coagulation, fibrinolysis, angiogenesis and osteogenesis. Depending on the composition of the protein layer, these activities may or may not be adequately carried out [25].

Doping the sol-gel coating (previously designed by our group [26]) with increasing percentages of Sr (0%, 0.5%, 1% and 1.5%) let us study the effect of this cation on the biological processes necessary for bone regeneration after medical procedures such as dental implantation. The coatings were characterised physiochemically, and the proteins adsorbed on the surfaces after their exposure to human serum were studied using proteomics. Moreover, *in vitro* cell responses were examined using the MC3T3-E1 osteoblasts and RAW 264.7 macrophages.

2. Materials and methods

2.1. Sol-gel synthesis and sample preparation

The synthesis of hybrid sol-gel coatings was performed using the combination of two silica precursors with different organic functional groups, namely, methyltrimethoxysilane (MTMOS; M) and tetraethyl orthosilicate (TEOS; T). The molar percentages of these reagents were 70% of M and 30% of T, as described in the previous studies [27]. To obtain the base coating, these alkoxysilanes were mixed in 2-propanol at a 1:1 vol ratio of alcohol to the precursor. The necessary stoichiometric quantity of 0.1 M HNO_3 was added drop-by-drop to hydrolyse the alkoxy groups in the precursors. The required amount of $SrCl_2$ was dissolved in this solution, which catalysed the reaction. To allow the sol-gel polymerisation, the mixtures were kept for 1 h under stirring, followed by 1 h at rest at room temperature. Four different compositions were synthesised: the coating without Sr (MT) and doped with 0.5, 1 and 1.5 wt% $SrCl_2$ (called MT0.5Sr, MT1Sr and MT1.5Sr, respectively). All the reagents were purchased from Sigma-Aldrich (St. Louis, MO, USA). Immediately after the synthesis, the obtained sol-gels were applied onto different substrates, depending on the test to be performed. The discs (10-mm and 12-mm diameter and 1.2-mm thickness) of grade 4 commercially pure Ti, with the sandblasted and acid-etched surface (SAE), were purchased from GMI-Ilerimplant S.L. (Lleida, Spain). They were coated using a dip coater (ND-DC 11/1 150, Nadetech Innovations S.L., Navarra, Spain) at an immersion speed of 60 mm min^{-1}, with a pause of 1 min and a withdrawal speed of 100 mm min^{-1}. To obtain the samples for the hydrolytic degradation and Sr^{2+} release studies, glass slides were coated by casting. Before coating, the surfaces were cleaned with an HNO_3 solution (25%, w/w) in an ultrasonic bath (Ultrasons-P, JP Selecta, Barcelona, Spain) for 15 min. Afterwards, they were cleaned and sonicated in distilled water. For the chemical characterisation of the materials, each sol was poured into a Teflon mould (Mecanizados Suguz S.L., Andoain, Spain) to obtain free films. Subsequently, the samples were cured at 80 °C for 2 h.

2.2. Physicochemical characterisation

The surface topography of the samples was examined employing scanning electron microscopy (SEM). Leica-Zeiss LEO 440 microscope was used, acquiring the images at a voltage of 15 kV. A Sputter Coater (SCD500, BALTEC, Pfäffikon, Switzerland) was employed to form a fine platinum coat on the sample. To characterise the roughness of the biomaterials, an optical profilometer (Veeco Instruments Inc., Plainview, NY, USA) was used. Three measurements were taken for each synthesised material, and the Ra values were calculated. The wettability was determined by measuring the contact angle of ultrapure water on different surfaces, using an automatic goniometer (OCA 20, DataPhysics Instruments GmbH, Filderstadt, Germany). The test was carried out at room temperature after placing a sessile drop of 10 μL on the coated surfaces. Five discs of each material were examined, with two drops deposited on each disc. Hydrolytic degradation of the coatings was evaluated by gravimetric measurements, comparing the weight of the samples before and after soaking in 50 mL of distilled water, at 37 °C, for 1, 2, 4, 6 and 8 weeks. Each data point represents the average of three measurements. The amount of Sr^{2+} released to the media during the degradation of the network was evaluated using inductively coupled plasma atomic emission spectroscopy (ICP-AES) (Activa, Horiba Jobin Yvon IBH Ltd., Glasgow, UK). The coatings were immersed in 50 mL of ultrapure water at 37 °C. After 2, 4, 8, 24, 72, 168, 336, 504 and 672 h of immersion, a 500-μL sample was removed, and the Sr^{2+} concentration was determined. Measurements were performed in triplicate. The siloxane network formed in coatings was studied using Fourier-transform infrared spectroscopy (FTIR), employing an attenuated total reflection system (ATR) (Nicolet 6700, Thermo Fisher Scientific, Waltham, MA, USA). The transmission spectra were obtained in the range of 4000–600 cm^{-1} (corresponding to the mid-infrared region). The final structure of the siloxane network and the Si-O-Si crosslinking density were characterised using solid-state ^{29}Si-NMR spectroscopy. The spectra were recorded employing a Bruker 400 Avance III WB PLUS spectrometer at 79.5 MHz.

2.3. In vitro assays

2.3.1. Cell culture

MC3T3-E1 (mouse calvaria osteosarcoma) and RAW 264.7 (mouse murine macrophage) cells were cultured on the coated discs in 48-well NUNC plates in DMEM (Gibco, Thermo Fisher Scientific) with 10% FBS (Gibco) and 1% penicillin/streptomycin (Biowest Inc., Riverside, MO, USA). The cells were incubated for 24 h at 37 °C in humidified (95%) CO_2 atmosphere. Then, the medium in MC3T3-E1 wells was replaced with the osteogenic medium composed of DMEM, 1% of penicillin/streptomycin, 10% FBS, 1% ascorbic acid (5 mg mL^{-1}) and 0.21% β-glycerol phosphate. This medium was changed every 48 h.

2.3.2. Cytotoxicity, proliferation and ALP activity

The cytotoxicity was evaluated following the ISO 10993-5 norms. Cytotoxicity was calculated following the formula $CVsample \times 100/CVblank$, where CV is the cell viability and blank refers to the cells seeded without any material. Proliferation capability was examined using a Cell Titer Proliferation Assay kit (Promega, Madison, WI, USA), according to the manufacturer's directions. A culture without titanium discs was used as a negative control, and cells incubated with latex constituted a positive control. The material was considered cytotoxic if the cell viability was reduced to less than 70% of control levels within the examined period.

To assess cell proliferation on the synthesised coatings (after 1, 3 and 7 days), the AlamarBlue™ Cell Viability Reagent (Invitrogen, Thermo Fisher Scientific) was used, following the manufacturer's protocol. Cell proliferation was calculated as $((O2xA1) - (O1xA2)/(R1xN2) - (R2xN1))x100$, where O1 is the molar extinction coefficient (E) of oxidised AlamarBlue at 570 nm, O2 is the E of oxidised AlamarBlue at

620 nm, R1 is the E of AlamarBlue reduced at 570 nm, R2 is the E of AlamarBlue reduced at 620 nm, A1 is the sample absorbance at 570, A2 is the sample absorbance at 620 nm, N1 is the negative control (cell culture medium without cells) at 570 nm and N2 is the negative control absorbance at 620 nm.

The alkaline phosphatase activity was measured using the method of Araújo-Gomes et al. [28]. The MC3T3-E1 cells were cultured on the biomaterials for 7 and 14 days; then, the conversion of p-nitrophenylphosphate to p-nitrophenol was used to assess the activity of the enzyme. The data were expressed as ALP activity normalised to the total protein content (obtained using a Pierce BCA Assay kit (Thermo Fisher Scientific)).

2.3.3. Quantitative real-time PCR

To evaluate the effects of the Sr-doped biomaterials on gene expression, the MC3T3-E1 cells were cultured with the coated discs for 7 and 14 days, and the RAW264.7 for 2 and 4 days. There were six replicate cultures for each type of coating. RNA was isolated using TRIzol and transformed to cDNA as described by Cerqueira et al. [29]. The sequences employed for the gene amplification were as follows:

ALP-F: CCAGCAGGTTTCTCTCTTGG, ALP-R: CTGGGAGTCTCATCCTGAGC, TGF-β-F: TTGCTTCAGCTCCACAGAGA, TGF-β-R: TGGTTGTAGAGGGCAAGGAC, TNF-α-F: AGCCCCCAGTCTGTATCCTT and TNF-α-R: CTCCCTTTGCAGAACTC.

GAPDH was used to normalise the obtained data and as an endogenous control. The PCR reactions were carried out using SYBR Premix Ex Taq (Tli RNase H Plus) (Takara Bio Inc., Kusatsu, Japan). A StepOnePlus Real-Time PCR system (Applied Biosystems, Foster City, CA, USA) was employed, as described by Cerqueira et al. [30].

2.3.4. Cytokine quantification using enzyme-linked immunosorbent assay (ELISA)

Tumour necrosis factor-alpha (TNF-α) was quantified in the media used to culture the RAW 264.7 cells in contact with the studied materials. After 2 and 4 days of culture, the medium was collected and frozen until further analysis. The TNF-α concentration was determined using an ELISA kit (Thermo Fischer Scientific), following the manufacturer's instructions.

2.4. Adsorbed protein layer and proteomic analysis

To obtain the proteins adsorbed on the surfaces, Sr-doped and non-doped biomaterials were incubated for 3 h with 1 mL of human blood serum from male AB plasma (Sigma-Aldrich) in 24-well NUNC plates (37 ºC, 5% CO_2). To eliminate non-adsorbed proteins, the discs were washed 5 times with ddH_2O and once with 100 mM NaCl, 50 mM Tris-HCl, pH 7. The final elution was performed by immersing the disks in 4% SDS and 100 mM DTT solution in 0.5 M triethylammonium bicarbonate buffer (TEAB; Sigma-Aldrich).

Four independent replicates were analysed for each surface type; each replicate was obtained by pooling the eluates from 4 discs. Before the test, the protein in the serum was quantified using a Pierce BCA Assay kit (Thermo Fisher Scientific).

The protocol described by Romero-Gavilán et al. [31] was followed for proteomic analysis. The proteins were characterised using liquid chromatography-tandem mass spectrometry (LC-MS/MS), employing a nanoACQUITY UPLC (Waters, Milford, MA, USA) system with an Orbitrap XL (Thermo Electron, Bremen, Germany). Progenesis QI software (Nonlinear Dynamics, Newcastle, UK) was used to perform differential analysis of identified proteins, and the functional classification was performed employing UniProt tools [32].

2.5. Statistical analysis

Data were subjected to one-way analysis of variance (ANOVA) and a Newman-Keuls multiple comparison post-hoc test. Differences between MT (control) and the doped coatings with different Sr concentrations were considered statistically significant at $p \leq 0.05$ (*), $p \leq 0.01$ (**) and $p \leq 0.001$ (***).

3. Results

3.1. Physicochemical characterisation

The hybrid sol-gel coatings were successfully synthesised. They adhered to the Ti discs well, without phase separation or precipitates of $SrCl_2$, as can be seen in the SEM micrographs (Fig. 1**a–d**). The samples with a higher percentage of salt, examined at high magnifications, show small porosities of about 100 nm (Fig. 1**e–f**). These pores were probably formed by the evaporation of volatile compounds trapped within the coating [33].

The synthesised sol-gel materials covered the initial roughness of the Ti discs, leading to a decrease in the average surface roughness, Ra (Fig. 2**a**). The value of Ra increased slightly as greater amounts of Sr were incorporated. However, these differences were not significant in Newman-Keuls tests of multiple comparisons.

Coating with the MT base material strongly raises the hydrophilicity of titanium, resulting in a contact angle of around 50º (Fig. 2**b**). Doping the coatings with $SrCl_2$ causes a considerable increase in the contact angle, to approximately 75º. The doped materials are more hydrophobic than the MT but still more hydrophilic than an uncoated titanium disc (independently of the percentage of Sr in the coating).

The Sr-containing coatings showed higher degradation rates than the MT (Fig. 3**a**); however, the differences between these coatings (0.5%, 1% and 1.5%) were small. For all three doping levels, a considerable loss of material is observed during the first seven days of the test, while later, the loss becomes less pronounced and more gradual. The base coating shows a similar tendency. Fig. 3**b** shows the kinetic liberation of Sr^{2+}. The three coatings have similar profiles, with a very quick release in the first 2 h of the test, followed by an almost steady state (with the total Sr loss depending on its initial concentration, i.e., 0.72 mg for MT1.5Sr, 0.43 mg for MT1Sr and 0.11 mg for MT0.5Sr).

The effect of $SrCl_2$ on the sol-gel structure was studied using FTIR and ^{29}Si-NMR. The region associated with the Si-O-Si bonds of the formed network (between 600 and 1200 cm^{-1}) was detected in all FTIR spectra (Fig. 4**a**). The signals seen at 1165, 1075 and 760 cm^{-1} confirm that polysiloxane networks were obtained in all cases [34]; Sr-doping does not negatively affect their formation. The band associated with Si-OH terminal groups can be seen at 940 cm^{-1}. Its intensity in all spectra is low, showing that few silanol groups failed to condense; the formed network was dense. The non-hydrolysable methyl groups of the MTMOS were observed as the peaks at 2975 and 1275 cm^{-1} [35]. These results were confirmed by the ^{29}Si-NMR spectra (Fig. 4**b**), where the strongest-intensity peaks corresponded to the species with a high degree of condensation, although the compaction of the network diminished slightly with increasing Sr content. These data show that the heat treatment promotes a dense crosslinked network, not significantly affected by the incorporation of the Sr salt at any of the examined concentrations.

3.2. In vitro assays

3.2.1. Effects on osteoblasts (osteogenic response)

In all cases, the cells cultured with the tested formulations had viability greater than 70% in comparison with the controls (Fig. 5**a**); none of the materials was cytotoxic. The results of proliferation tests were very similar, without significant differences (Fig. 5**b**).

Among the osteogenic gene markers detected by PCR, the ALP results for the MT0.5Sr coating (after 14 days of culture) stand out (Fig. 6**a**). TGF-β genes were overexpressed after 14 days of contact with 0.5%-Sr material (Fig. 6**b**).

The ALP activity was similar for all surfaces after 7 days of culture

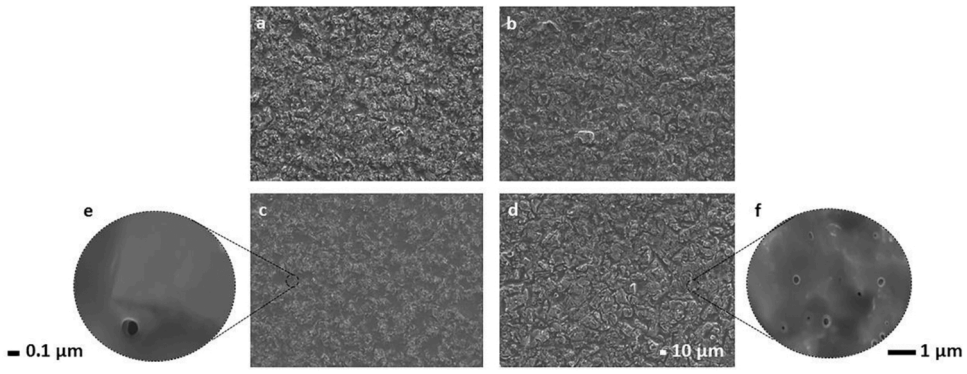

Fig. 1. SEM micrographs of MT (a), MT0.5Sr (b), MT1Sr (c), MT1.5Sr (d); × 300. Enlarged areas of MT1Sr (e; × 80,000) and MT1.5Sr (f; × 20,000) coatings. Scale bars: (a-d) 10 µm, (e) 0.1 µm and (f) 1 µm.

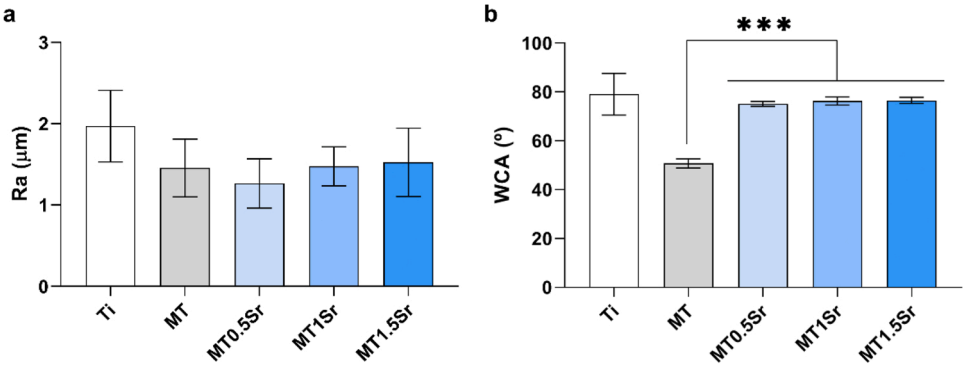

Fig. 2. Roughness (a) and contact angle (b) results. Results are shown as means ± SE. The asterisks ($p \leq 0.001$ (***)) indicate the statistical significance of differences between MT and Sr-doped MT.

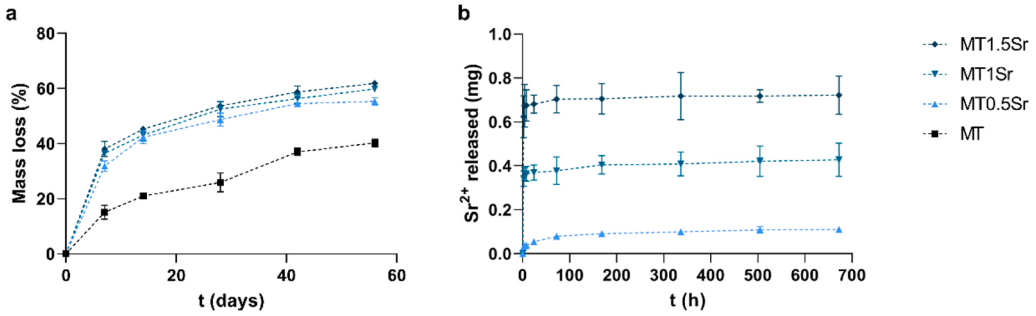

Fig. 3. Hydrolytic degradation (a) and kinetic liberation of Sr^{2+} (b) for the sol-gel coatings. Bars indicate standard errors.

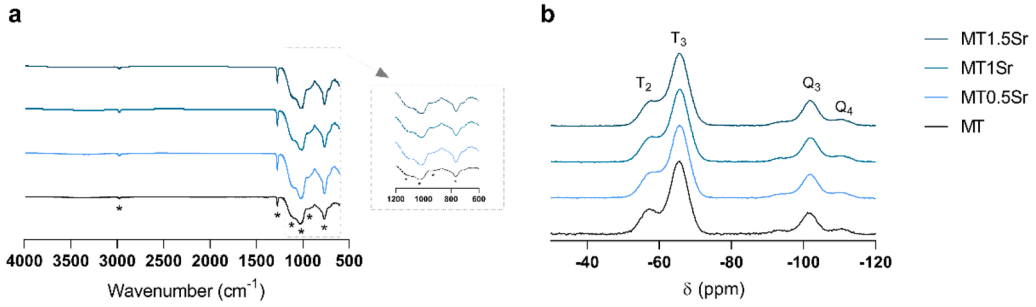

Fig. 4. FTIR (a) and ^{29}Si-NMR (b) spectra of sol-gel networks MT, MT0.5Sr, MT1Sr and MT1.5Sr.

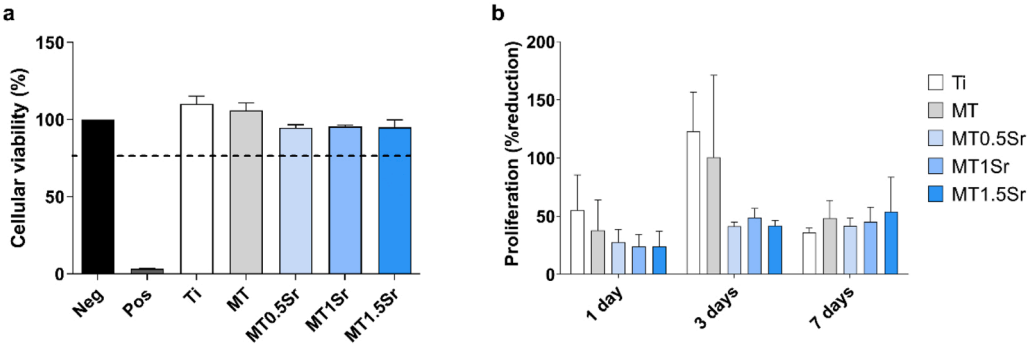

Fig. 5. MC3T3-E1 cell viability (a) and proliferation (b). Results are shown as means ± SE.

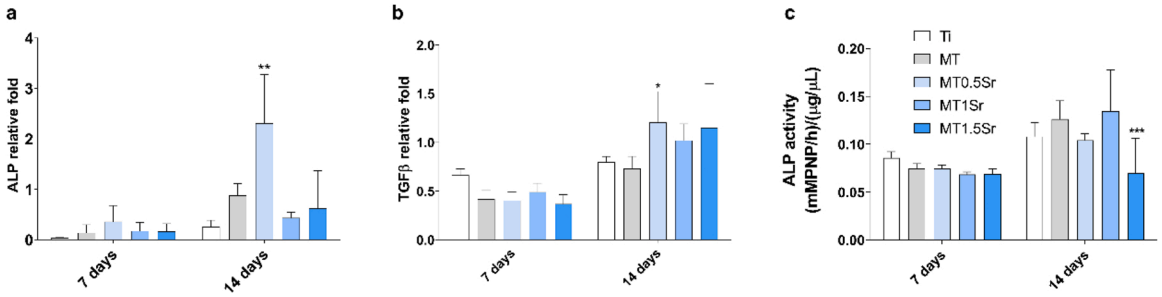

Fig. 6. Gene expression of ALP (a), TGF-β (b) and ALP activity (c) in MC3T3-E1 cultures after 7 and 14 days. Results are shown as means ± SE. The asterisks ($p \leq 0.05$ (*), $p \leq 0.01$ (**) and $p \leq 0.001$ (***)) indicate the statistical significance of differences between MT and Sr-doped MT.

(Fig. 6**c**). In contrast, after 14 days, the cells grown with materials containing 1.5% of Sr showed a significant decrease in the activity of this enzyme.

3.2.2. *Effects on macrophages (inflammatory response)*

Macrophages cultured with Ti-control discs showed raised levels of inflammation in comparison with the cells exposed to the coated discs (after 2 and 4 days, Fig. 7**a**), reflected by elevated TNF-α gene expression. The inflammation levels after 2 days were higher for the cells incubated with discs with larger percentages of Sr than for the MT material (the differences were statistically significant for MT1Sr and MT1.5Sr). However, after 4 days of incubation, the inflammation indicators clearly decreased in MT1Sr samples.

Changes in the expression of TGF-β (Fig. 7**b**) indicate anti-inflammatory activity associated with the incorporation of Sr (after 2 and 4 days); the TGF-β expression values are higher for the Sr-doped coatings than for the MT material.

The level of pro-inflammatory marker TNF-α examined using ELISA (Fig. 7**c**) decreases for the coatings doped with 0.5% and 1% Sr after 2 days and for all compositions with Sr after 4 days of culture. Moreover, uncoated titanium has a higher inflammatory potential than coated discs.

3.3. *Proteomic analysis*

The LC-MS/MS analysis identified 111 proteins adsorbed to the studied surfaces (Supplementary Table 1), of which 46 differed in their affinity to the studied materials compared to MT (statistically significant differences, Progenesis QI differential analysis). A group of 6 proteins (Table 1) decreased their adsorption levels when $SrCl_2$ was added to the sol-gel network. In contrast, 40 proteins tended to increase their affinity and adsorbed to the surfaces of Sr-doped materials in greater proportions than to MT (Table 2).

Among the 40 proteins with increased adsorption, several were associated with the immune system (C1S, C1R, CO3, C4BPA, CFAH, IC1 and immunoglobulins IGLL5, IGHG1 and KV302). Moreover, some proteins related to blood coagulation and fibrinolysis processes were identified (A2MG, FA11, FA5, HRG, KNG1, PROS and THBR). In fact, the HRG protein is at the top of the list for the formulation containing 1.5% Sr, where it is 11.2 times more abundant than in the reference sample. However, the levels of ANT3 and PROC, linked to the inhibition of coagulation, were reduced on doped coatings. Apolipoproteins APOA2,

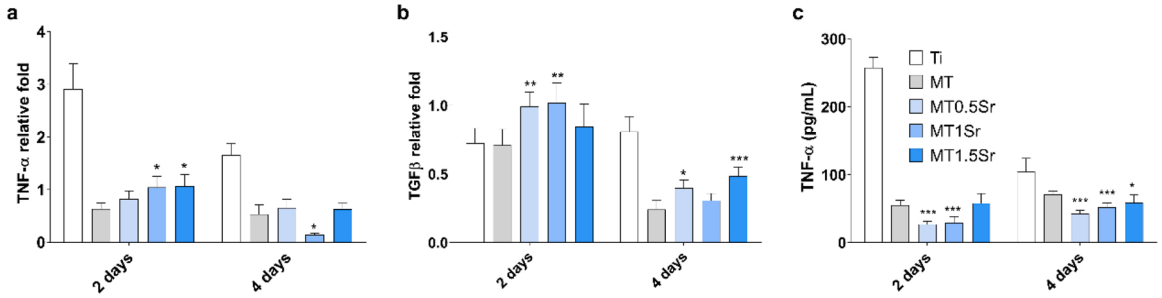

Fig. 7. Gene expression of TNF-α (a), TGF-β (b) and TNF-α ELISA in RAW264.7 macrophages after 2 and 4 days of culture. Results are shown as means ± SE. The asterisks ($p \leq 0.05$ (*), $p \leq 0.01$ (**) and $p \leq 0.001$ (***)) indicate the statistical significance of differences between MT and Sr-doped MT.

Table 1
Progenesis comparative analysis of proteins differentially adsorbed onto Sr-enriched coatings respect base material. Detected proteins with ANOVA $p < 0.05$ (yellow) and a ratio lower than 0.77 (red) were considered as significantly different (bold).

		MT0.5Sr vs MT		MT1Sr vs MT		MT1.5Sr vs MT	
Code	**Protein**	***p***	**Ratio**	***p***	**Ratio**	***p***	**Ratio**
APOD	Apolipoprotein D	**0.017**	**0.75**	0.207	0.79	0.197	0.89
A1AG1	Alpha-1-acid glycoprotein 1	0.821	1.23	0.533	1.38	**0.043**	**0.59**
A1AG2	Alpha-1-acid glycoprotein 2	0.947	1.13	0.553	1.35	**0.027**	**0.57**
ZA2G	Zinc-alpha-2-glycoprotein	0.681	0.96	0.485	0.86	**0.006**	**0.53**
ANT3	Antithrombin-III	**0.019**	**0.19**	0.463	0.62	0.096	0.35
PROC	Vitamin K-dependent protein C	**0.011**	**0.41**	0.006	0.14	**0.006**	**0.35**

APOC1, APOC4, APOH, APOL1 and the high-density apolipoprotein SAA4 were more abundant on the materials doped with Sr than without doping. However, the APOD protein showed reduced affinity to these surfaces. The glycoproteins ITIH4 and SEPP1 were found on the Sr-doped materials, while A1AG1, A1AG2, and ZA2G glycoproteins showed preferential bonding to MT. Finally, TETN, GELS, PON1 and PCOC1, the proteins related to bone regeneration, were also more common on 1%-Sr coatings.

Fig. 8 shows the Sr-content-dependent changes in the normalised abundance of 15 proteins involved in inflammation (blue), coagulation (red), fibrinolysis (green) and bone regenerative processes (orange).

4. Discussion

The aim of this study was to examine the effect of the Sr cation incorporated in sol-gel coatings on the early biological bone regeneration processes.

Adding Sr to the sol-gel network changes the physicochemical characteristics of the surface of the base material without modifying the adhesion of the coating. The incorporation of Sr did not affect the final network crosslinking but modified the wettability of the surface (Fig. 2). Increasing the amount of Sr in the sol-gels resulted in materials of a more hydrophobic character. These coatings have a contact angle of around 70º. Interestingly, this is the value described as the optimal contact angle for cell adhesion [36], an important initial process in good tissue response. Regarding hydrolytic degradation (Fig. 3**a**), the materials with $SrCl_2$ show higher percentages of degradation than the MT. This agrees with previous results obtained by our group [37]. Degradation levels higher than 50% are observed after 8 weeks. The degradation of the sol-gel coatings is caused by a well-known hydrolysis process [38], which results in the release of the incorporated salt. The more Sr incorporated into the coating, the more was liberated (Fig. 3**b**). A rapid release observed in the first hours was followed by a progressive stabilisation until the end of the experiment, reaching the value of 0.7 mg for the MT1.5Sr. Thus, this study confirms the ability of these coatings to release doping agents to fulfil their osteoregenerative function.

The modifications in the physicochemical properties of the different formulations affect the abundance and distribution of the deposited proteins. The cellular behaviour will also be affected by these changes. Furthermore, none of the synthesised materials is cytotoxic.

The immune response is primarily driven by the proteins of the complement system. This is activated by different pathways (classical, lectin and alternative), following a sequence of events until finally triggering the inflammatory response. The expression of TNF-α gene in the macrophage cell culture with Sr-doped materials (after 2 days) is higher than in the cells in contact with the base coating. Similarly, the TGF-β inflammatory regulatory gene shows an increased expression after 2 days, in a Sr-dose-dependent manner. After 4 days, however, the expression of TNF-α decreases for the 1%-Sr material. At the same time, the TGF-β expression is still higher than in the MT samples. This remarkable observation indicates that the inflammation does not become chronic. In the ELISA test, the values for the pro-inflammatory marker TNF-α (principal pro-inflammatory cytokine secreted by the immune system by cells like macrophages) for doped materials decreased in comparison with the base coating. The proteomic analysis showed that the higher the content of Sr, the bigger increase in pro-inflammatory protein levels (such as C1S, C1R or CO3). Protein adhesion to the surface of a biomaterial might initiate an immune/inflammatory reaction *in vivo* [39]. Specifically, the CO3 can be linked to an immune and inflammatory response via its involvement in the activation of the complement cascade [40]. In contrast, the C4BPA, IC1 and the CFAH, adhering in large amounts to the MT1Sr, can inhibit the activation of this cascade [39,41]. C4BPA restricts the activation of this pathway, regulating its intensity [42], thus modulating the immune/inflammatory response to achieve a correct tissue regeneration [43]. However, if this process is not regulated, chronic inflammation could occur due to a disproportionate immune reaction, leading to implant failure [44]. Furthermore, IC1 controls the activation of the C1 complex. It forms a proteolytically inactive stoichiometric complex with the C1r or C1s proteases [45]. Apolipoproteins, such as the APOC4, could also play a role in preventing the activation of the innate immune response [46]. The inhibitory proteins seem to have a stronger effect than the initiators; at the beginning, the presence of Sr increases the inflammation, which is eliminated later.

Coagulation is an important process, and its development is key to bone regeneration. The process can be activated in two ways, intrinsic and extrinsic, which converge into the common pathway. This is linked to the complement system, creating a cooperative and highly beneficial union. There are several proteins whose levels increase with the Sr incorporation in the coating: FA11, FA5, THRB and KNG1. The FA11 and THRB participate in the initiation of this pathway. The THRB can trigger blood clotting through its conversion to thrombin protease, activating platelet formation [47]. The FA5 has a regulatory function in the pro- and anti-coagulant pathways [48]. The high molecular weight KNG1

Table 2
Progenesis comparative analysis of proteins differentially adsorbed onto Sr-enriched coatings respect base material. Detected proteins with ANOVA $p < 0.05$ (yellow) and a ratio higher than 1.3 (green) were considered as significantly different (bold).

		MT0.5Sr vs MT		MT1Sr vs MT		MT1.5Sr vs MT	
Code	Protein	*p*	Ratio	*p*	Ratio	*p*	Ratio
HRG	Histidine-rich glycoprotein	0.415	1.39	**0.010**	**9.51**	**0.020**	**11.23**
FA11	Coagulation factor XI	0.192	1.60	**0.000**	**9.09**	0.055	6.85
CADH1	Cadherin-1	0.498	1.83	**0.031**	**6.77**	0.302	5.27
PCOC1	Procollagen C-endopeptidase enhancer 1	0.210	5.04	**0.038**	**17.68**	0.156	4.06
KV302	Ig kappa chain V-III region SIE	0.059	3.39	**0.001**	**12.49**	0.561	4.06
KNG1	Kininogen-1	**0.021**	**1.95**	**0.005**	**4.19**	0.148	3.21
LAC2	Ig lambda-2 chain C regions	0.238	2.09	**0.006**	**7.23**	0.402	2.92
APOC1	Apolipoprotein C-I	**0.031**	**2.37**	**0.018**	**2.43**	0.103	2.77
APOC4	Apolipoprotein C-IV	**0.004**	**1.93**	**0.021**	**1.85**	**0.003**	**2.71**
TETN	Tetranectin	**0.036**	**2.16**	**0.006**	**3.59**	0.221	2.53
CD5L	CD5 antigen-like	**0.004**	**2.53**	**0.001**	**3.32**	0.057	2.50
PROS	Vitamin K-dependent protein S	**0.001**	**2.84**	**0.007**	**3.75**	0.088	2.35
APOL1	Apolipoprotein L1	**0.001**	**1.93**	**0.029**	**1.55**	**0.001**	**2.32**
SEPP1	Selenoprotein P	0.055	1.47	**0.015**	**1.87**	**0.010**	**2.28**
C4BPA	C4b-binding protein alpha chain	**0.002**	**2.59**	**0.002**	**2.89**	**0.031**	**2.23**
HV320	Ig heavy chain V-III region GAL	**0.002**	**2.66**	**0.000**	**3.08**	0.460	2.20
GELS	Gelsolin	**0.022**	**2.01**	**0.003**	**4.01**	0.110	2.19
SAA4	Serum amyloid A-4 protein	0.387	1.12	0.693	1.09	**0.001**	**2.14**
CFAH	Complement factor H	0.087	1.46	**0.006**	**3.22**	**0.033**	**2.08**
IGLL5	Immunoglobulin lambda-like polypeptide 5	0.259	1.77	**0.008**	**4.14**	0.274	2.07
AMBP	Protein AMBP	0.402	1.26	**0.017**	**3.35**	0.219	1.96
APOH	Beta-2-glycoprotein 1	0.107	2.79	**0.040**	**6.15**	0.917	1.88
HEMO	Hemopexin	0.144	1.82	**0.019**	**4.00**	0.434	1.83
FA5	Coagulation factor V	0.078	1.96	**0.038**	**2.42**	0.278	1.71
IGHG1	Ig gamma-1 chain C region	**0.017**	**1.95**	**0.036**	**2.88**	0.218	1.68
CO3	Complement C3	0.073	1.59	**0.016**	**2.36**	0.469	1.55
A1AT	Alpha-1-antitrypsin	0.066	1.85	**0.005**	**3.69**	0.307	1.54
PPIB	Peptidyl-prolyl cis-trans isomerase B	0.395	1.53	**0.019**	**4.91**	0.488	1.52
AACT	Alpha-1-antichymotrypsin	0.094	1.73	**0.002**	**3.87**	0.155	1.52
THRB	Prothrombin	0.411	1.13	0.097	1.36	**0.036**	**1.52**
IC1	Plasma protease C1 inhibitor	**0.000**	**1.79**	**0.001**	**2.16**	0.165	1.49
ITIH4	Inter-alpha-trypsin inhibitor heavy chain H4	0.126	1.29	**0.034**	**1.98**	0.058	1.47
C1R	Complement C1r subcomponent	**0.004**	**1.65**	**0.020**	**1.41**	**0.009**	**1.45**
APOA2	Apolipoprotein A-II	**0.023**	**1.45**	0.682	1.07	0.050	1.32
KV105	Ig kappa chain V-I region DEE	0.166	1.29	**0.038**	**1.97**	0.444	1.25
HPT	Haptoglobin	0.127	2.08	**0.011**	**3.63**	0.775	1.20
ITIH1	Inter-alpha-trypsin inhibitor heavy chain H1	0.086	1.79	**0.045**	**2.84**	0.766	1.16
PON1	Serum paraoxonase / arylesterase 1	0.056	1.38	**0.044**	**1.81**	0.693	1.12
C1S	Complement C1s subcomponent	**0.049**	**1.39**	0.417	1.12	0.681	1.06
A2MG	Alpha-2-macroglobulin	0.458	1.43	**0.039**	**2.32**	0.999	1.00

belongs to the kallikrein-kinin system and is involved in the intrinsic coagulation pathway [49]. In contrast, the levels of other coagulation regulatory proteins, ANT3 and PROC, decrease with the incorporation of strontium in the coatings. The PROC protein is involved in regulating the coagulation pathway, inactivating factors Va and VIIIa and, later, controlling the generation of thrombin [50]. Similarly, the ANT3 can regulate thrombin formation by inhibiting FIIa and FXa [51]. Thus, more proteins related to coagulation function are found on the doped coatings than on untreated surfaces. Therefore, we can suggest that the addition of Sr improves the functioning of the coagulation system.

The fibrinolytic system is complex, and it is intrinsically related to the blood coagulation system; it degrades the fibrin networks formed in the coagulation process, preventing thrombi formation. The levels of HRG protein, associated with the regulation of fibrinolysis [52], are elevated on the most doped surfaces. This protein interacts with plasminogen and fibrinogen [53]; it modulates functions related to the coagulation system. Tsuchida-Straeten et al. have reported an improvement in fibrinolysis in mice lacking this protein [54].

Osteogenesis is the process of forming new bone tissue. A large number of proteins that play important roles in the osteoblast cellular response and the consequent differentiation are involved in this process. Increased gene expression of the osteogenic markers ALP and TGF-β was observed in the osteoblast cell line cultured with the Sr-doped materials, particularly the MT0.5Sr.

Verberckmoes et al. have also found that Sr increases the ALP gene expression [14], and Choudhary et al. have reported that strontium ranelate significantly enhances the ALP activity, osteoblastic differentiation and mineralisation [55]. A study by Nardone et al. has indicated that treatment with Sr^{2+} ions improves cell proliferation and osteogenic differentiation through the expression of ALP, asserting that this cation induces bone regeneration [56]. Kong et al. report that 14-day exposure to Sr increases TGF-β expression in osteoblasts, suggesting its active role in the bone cell metabolism and activity [57].

In our study, the ALP test (in the MC3T3 cell line) showed an increase in its activity within the interval of 1 to 2 weeks. The highest activity was observed for the coating with 1% of Sr, coinciding with the maximum normalised abundance of the proteins linked to bone regeneration (TETN, GELS, PCOC1 and PON1). Wewer et al. have studied the role of the TETN protein in bone formation in mammals, concluding that it is very important in mineralisation during osteogenesis [58]. This protein can bind to plasminogen and stimulate its activation, essential for regulating bone tissue formation [59]. The TETN also binds to calcium and heparin and could be an integral component of the bone matrix [60]. Iba et al. have investigated the role of TETN in bone fracture repair using two models of bone regeneration in mice lacking this protein. They have observed a delay in the regeneration of fractures and proposed that TETN might improve bone fracture regeneration [61].

A study by Dowling et al. has suggested that elevated levels of PON1 in human serum represent a protective mechanism against the effects of oxidative stress on bone formation associated with osteoclastic resorption [62]. Moreover, Thouverey et al. have pointed out that the GELS protein can promote the release of osteoblast matrix vesicles involved in initiating bone mineralisation [63]. Furthermore, the PCOC1 protein, associated with collagen biosynthesis and its binding [64], could be involved in forming the extracellular matrix and osseointegration. Thus, the observed increase in the affinity of these proteins to Sr-containing coatings might positively affect osteogenesis.

5. Conclusion

The results obtained in this study show that $SrCl_2$ can be successfully incorporated into the polysiloxane network, modifying the properties of the base coating. Both the osteoblast and macrophage cell lines cultured with the doped materials change their behaviour in a Sr-concentration-dependent manner, demonstrating their osteogenic potential and effect on anti-inflammatory response. The LC-MS/MS analysis reveals that the

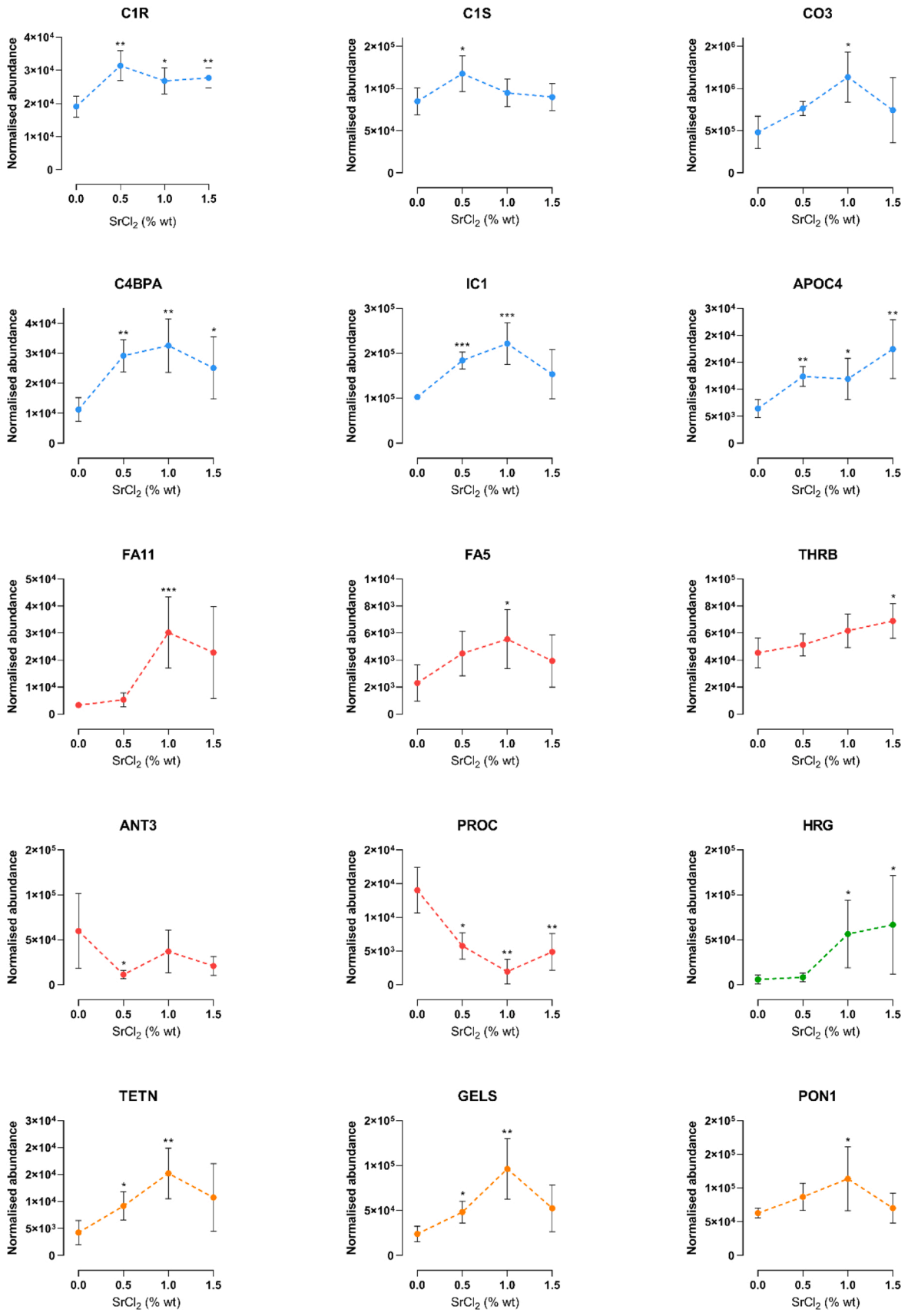

Fig. 8. The normalised abundance of the main 15 proteins (ANOVA: $p \leq 0.05$ (*), $p \leq 0.01$ (**) and $p \leq 0.001$ (***)).

presence of Sr modifies the adhesion profiles of proteins involved in inflammation, coagulation, bone regeneration or fibrinolysis processes. These observations show that adding Sr to biomaterials can improve their anti-inflammatory and osteogenic potential and positively affect the coagulation system.

CRediT authorship contribution statement

Iñaki García-Arnáez: Formal analysis, Investigation, Writing – original draft, Writing – review & editing. **Andreia Cerqueira**: Methodology, Investigation. **Francisco Romero-Gavilán**: Investigation, Writing – review & editing. **Félix Elortza**: Data curation, Writing – review & editing. **Mikel Azkargorta**: Investigation, Data curation. **Ibon Lloro**: Investigation, Data curation. **Julio Suay**: Conceptualization, Writing – review & editing, Funding acquisition. **Isabel Goñi**: Conceptualization, Writing – review & editing, Funding acquisition. **Mariló Gurruchaga**: Conceptualization, Writing – review & editing, Funding acquisition.

Declaration of Competing Interest

The authors declare that they have no known competing financial interests or personal relationships that could have appeared to influence the work reported in this paper.

Data availability

Data will be made available on request.

Acknowledgements

The work was supported by MICIU [RTC-2017-6147-1], MINECO [PID2020-113092RB-C21], Generalitat Valenciana [APOSTD/2020/036, PROMETEO/2020/069], Basque Government [PRE_2016_1_0141] and Universitat Jaume I [UJI-B2021-25]. The authors would like to thank the company GMI-Ilerimplant for producing the titanium discs.

Appendix A. Supporting information

Supplementary data associated with this article can be found in the online version at doi:10.1016/j.mtcomm.2022.104674.

References

[1] M. Jiménez, C. Abradelo, J. San Román, L. Rojo, Bibliographic review on the state of the art of strontium and zinc based regenerative therapies. Recent developments and clinical applications, J. Mater. Chem. B 7 (2019) 1974–1985, https://doi.org/10.1039/c8tb02738b.

[2] S. Lymperi, N. Horwood, S. Marley, M.Y. Gordon, A.P. Cope, F. Dazzi, Strontium can increase some osteoblasts without increasing hematopoietic stem cells, Blood J. Am. Soc. Hematol. 111 (2008) 1173–1181.

[3] L. Mao, L. Xia, J. Chang, J. Liu, L. Jiang, C. Wu, et al., The synergistic effects of Sr and Si bioactive ions on osteogenesis, osteoclastogenesis and angiogenesis for osteoporotic bone regeneration, Acta Biomater. 61 (2017) 217–232.

[4] S. Zhu, X. Hu, Y. Tao, Z. Ping, L. Wang, J. Shi, et al., Strontium inhibits titanium particle-induced osteoclast activation and chronic inflammation via suppression of NF-κB pathway, Sci. Rep. 6 (2016) 1–11, https://doi.org/10.1038/srep36251.

[5] C. Zhou, A. Xu, D. Wang, G. Lin, T. Liu, F. He, The effects of Sr-incorporated micro/nano rough titanium surface on rBMSC migration and osteogenic differentiation for rapid osteointegration, Biomater. Sci. 6 (2018) 1946–1961.

[6] Z. Saidak, P.J. Marie, Strontium signaling: molecular mechanisms and therapeutic implications in osteoporosis, Pharmacol. Ther. 136 (2012) 216–226.

[7] I. Cacciotti, Bivalent cationic ions doped bioactive glasses: the influence of magnesium, zinc, strontium and copper on the physical and biological properties, J. Mater. Sci. 52 (2017) 8812–8831, https://doi.org/10.1007/s10853-017-1010-0.

[8] N. Neves, D. Linhares, G. Costa, C.C. Ribeiro, M.A. Barbosa, In vivo and clinical application of strontium-enriched biomaterials for bone regeneration, Bone Jt. Res. 6 (2017) 366–375, https://doi.org/10.1302/2046-3758.66.BJR-2016-0311.R1.

[9] F. Romero-gavilán, N. Araújo-gomes, I. García-arnáez, C. Martínez-ramos, F. Elortza, The effect of strontium incorporation into sol-gel biomaterials on their protein adsorption and cell interactions, Colloids Surf. B Biointerfaces 174 (2019) 9–16, https://doi.org/10.1016/j.colsurfb.2018.10.075.

[10] J.C. Almeida, A. Wacha, P.S. Gomes, L.C. Alves, M.H.V. Fernandes, I.M.M. Salvado, et al., A biocompatible hybrid material with simultaneous calcium and strontium release capability for bone tissue repair, Mater. Sci. Eng. C 62 (2016) 429–438, https://doi.org/10.1016/j.msec.2016.01.083.

[11] S. Omar, F. Repp, P.M. Desimone, R. Weinkamer, W. Wagermaier, S. Ceré, et al., Sol-gel hybrid coatings with strontium-doped 45S5 glass particles for enhancing the performance of stainless steel implants: electrochemical, bioactive and in vivo response, J. Non Cryst. Solids 425 (2015) 1–10, https://doi.org/10.1016/j.jnoncrysol.2015.05.024.

[12] Ł. John, M. Podgórska, J.M. Nedelec, Ł. Cwynar-Zajac, P. Dzięgiel, Strontium-doped organic-inorganic hybrids towards three-dimensional scaffolds for osteogenic cells, Mater. Sci. Eng. C 68 (2016) 117–127, https://doi.org/10.1016/j.msec.2016.05.105.

[13] P. Marie, Strontium ranelate in osteoporosis and beyond: identifying molecular targets in bone cell biology, Mol. Interv. 10 (2010) 305–312, https://doi.org/10.1124/mi.10.5.7.

[14] S.C. Verberckmoes, M.E. De Broe, P.C. D'Haese, Dose-dependent effects of strontium on osteoblast function and mineralization, Kidney Int. 64 (2003) 534–543, https://doi.org/10.1046/j.1523-1755.2003.00123.x.

[15] S.G. Dahl, P. Allain, P.J. Marie, Y. Mauras, G. Boivin, P. Ammann, et al., Incorporation and distribution of strontium in bone, Bone 28 (2001) 446–453, https://doi.org/10.1016/S8756-3282(01)00419-7.

[16] W. Zhang, H. Cao, X. Zhang, G. Li, Q. Chang, J. Zhao, et al., A strontium-incorporated nanoporous titanium implant surface for rapid osseointegration, Nanoscale 8 (2016) 5291–5301.

[17] H.Y. Lee, D. Lie, K.S. Lim, T. Thirumoorthy, S.M. Pang, Strontium ranelate-induced toxic epidermal necrolysis in a patient with post-menopausal osteoporosis, Osteoporos. Int. 20 (2009) 161–162, https://doi.org/10.1007/s00198-008-0677-0.

[18] I. Schrooten, G.J.S. Behets, W.E. Cabrera, S.R. Vercauteren, L.V. Lamberts, S. C. Verberckmoes, et al., Dose-dependent effects of strontium on bone of chronic renal failure rats, Kidney Int. 63 (2003) 927–935.

[19] K. Wang, C. Zhou, Y. Hong, X. Zhang, A review of protein adsorption on bioceramics, Interface Focus 2 (2012) 259–277, https://doi.org/10.1098/rsfs.2012.0012.

[20] S.A. Maskarinec, D.A. Tirrell, Protein engineering approaches to biomaterials design, Curr. Opin. Biotechnol. 16 (2005) 422–426, https://doi.org/10.1016/j.copbio.2005.06.009.

[21] A. Krishnan, C.A. Siedlecki, E.A. Vogler, Mixology of protein solutions and the Vroman effect, Langmuir 20 (2004) 5071–5078, https://doi.org/10.1021/la036218r.

[22] F. Romero-Gavilán, N.C. Gomes, J. Ródenas, A. Sánchez, M. Azkargorta, I. Iloro, et al., Proteome analysis of human serum proteins adsorbed onto different titanium surfaces used in dental implants, Biofouling 33 (2017) 98–111, https://doi.org/10.1080/08927014.2016.1259414.

[23] I. Lynch, Are there generic mechanisms governing interactions between nanoparticles and cells? Epitope mapping the outer layer of the protein-material interface, Phys. A Stat. Mech. Appl. 373 (2007) 511–520, https://doi.org/10.1016/j.physa.2006.06.008.

[24] I. Firkowska-Boden, X. Zhang, K.D. Jandt, Controlling protein adsorption through nanostructured polymeric surfaces, Adv. Health Mater. 7 (2018) 1–19, https://doi.org/10.1002/adhm.201700995.

[25] F. Romero-Gavilán, N. Araújo-Gomes, A. Cerqueira, I. García-Arnáez, C. Martínez-Ramos, M. Azkargorta, et al., Proteomic analysis of calcium-enriched sol–gel biomaterials, J. Biol. Inorg. Chem. 24 (2019) 563–574, https://doi.org/10.1007/s00775-019-01662-5.

[26] M. Martínez-Ibáñez, M.J. Juan-Díaz, I. Lara-Saez, A. Coso, J. Franco, M. Gurruchaga, et al., Biological characterization of a new silicon based coating developed for dental implants, J. Mater. Sci. Mater. Med. 27 (2016) 80.

[27] M. Martínez-Ibáñez, M.J. Juan-Díaz, I. Lara-Saez, A. Coso, J. Franco, M. Gurruchaga, et al., Biological characterization of a new silicon based coating developed for dental implants, J. Mater. Sci. Mater. Med. 27 (2016) 80, https://doi.org/10.1007/s10856-016-5690-9.

[28] N. Araújo-Gomes, F. Romero-Gavilán, I. García-Arnáez, C. Martínez-Ramos, A. M. Sánchez-Pérez, M. Azkargorta, et al., Osseointegration mechanisms: a proteomic approach, J. Biol. Inorg. Chem. 23 (2018) 459–470, https://doi.org/10.1007/s00775-018-1553-9.

[29] A. Cerqueira, F. Romero-Gavilan, N. Araujo-Gomes, I. Garcia-Arnaez, C. Martinez-Ramos, S. Ozturan, et al., A possible use of melatonin in the dental field: protein adsorption and in vitro cell response on coated titanium, Mater. Sci. Eng. C 116 (2020), 111262.

[30] A. Cerqueira, F. Romero-Gavilán, I. García-Arnáez, C. Martinez-Ramos, S. Ozturan, R. Izquierdo, et al., Characterization of magnesium doped sol-gel biomaterial for bone tissue regeneration: the effect of Mg ion in protein adsorption, Mater. Sci. Eng. C 125 (2021), 112114.

[31] F. Romero-Gavilan, A.M. Sánchez-Pérez, N. Araújo-Gomes, M. Azkargorta, I. Iloro, F. Elortza, et al., Proteomic analysis of silica hybrid sol-gel coatings: a potential tool for predicting the biocompatibility of implants in vivo, Biofouling 33 (2017) 676–689, https://doi.org/10.1080/08927014.2017.1356289.

[32] T.U. Consortium, UniProt: the universal protein knowledgebase in 2021, Nucleic Acids Res. 49 (2021) D480–D489.

[33] T.T. Phan, F. Bentiss, C. Jama, Effects of sol–gel process parameters on the anticorrosive performance of phosphosilicate hybrid coatings for carbon steel: structural and electrochemical studies, New J. Chem. 42 (2018) 13442–13452.

[34] A. Jitianu, A. Britchi, C. Deleanu, V. Badescu, M. Zaharescu, Comparative study of the sol-gel processes starting with different substituted Si-alkoxides, J. Non Cryst. Solids 319 (2003) 263–279, https://doi.org/10.1016/S0022-3093(03)00007-3.

[35] Y.Q. Yang, L. Liu, J.M. Hu, J.Q. Zhang, C.N. Cao, Improved barrier performance of metal alkoxide-modified methyltrimethoxysilane films, Thin Solid Films 520 (2012) 2052–2059, https://doi.org/10.1016/j.tsf.2011.10.041.
[36] C. Zolkov, D. Avnir, R. Armon, Tissue-derived cell growth on hybrid sol-gel films, J. Mater. Chem. 14 (2004) 2200–2205, https://doi.org/10.1039/b401715n.
[37] I. García-Arnáez, B. Palla, J. Suay, F. Romero-Gavilán, L. García-Fernández, M. Fernández, et al., A single coating with antibacterial properties for prevention of medical device-associated infections, Eur. Polym. J. (2019) 113, https://doi.org/10.1016/j.eurpolymj.2019.02.002.
[38] P. Saravanapavan, J.R. Jones, R.S. Pryce, L.L. Hench, Bioactivity of gel–glass powders in the CaO-SiO2 system: a comparison with ternary (CaO-P2P5–SiO2) and quaternary glasses (SiO2–CaO-P2O5–Na2O), J. Biomed. Mater. Res. Part A J. Soc. Biomater. Jpn. Soc. Biomater. Aust. Soc. Biomater. Korean Soc. Biomater. 66 (2003) 110–119.
[39] D. Ricklin, G. Hajishengallis, K. Yang, J.D. Lambris, Complement: a key system for immune surveillance and homeostasis, Nat. Immunol. 11 (2010) 785–797, https://doi.org/10.1038/ni.1923.
[40] A. Sahu, J.D. Lambris, Structure and biology of complement protein C3, a connecting link between innate and acquired immunity, Immunol. Rev. 180 (2001) 35–48.
[41] U. Kishore, R.B. Sim, Factor H as a regulator of the classical pathway activation, Immunobiology 217 (2012) 162–168.
[42] T.E. Mollnes, M. Kirschfink, Strategies of therapeutic complement inhibition, Mol. Immunol. 43 (2006) 107–121.
[43] Z. Chen, T. Klein, R.Z. Murray, R. Crawford, J. Chang, C. Wu, et al., Osteoimmunomodulation for the development of advanced bone biomaterials, Mater. Today 19 (2016) 304–321.
[44] A. Vishwakarma, N.S. Bhise, M.B. Evangelista, J. Rouwkema, M.R. Dokmeci, A. M. Ghaemmaghami, et al., Engineering immunomodulatory biomaterials to tune the inflammatory response, Trends Biotechnol. 34 (2016) 470–482.
[45] K.S. Aulak, A.E. Davis III, V.H. Donaldson, R.A. Harrison, Chymotrypsin inhibitory activity of normal C1–inhibitor and a P1 Arg to His mutant: evidence for the presence of overlapping reactive centers, Protein Sci. 2 (1993) 727–732.
[46] N. Cho, S. Seong, Apolipoproteins inhibit the innate immunity activated by necrotic cells or bacterial endotoxin, Immunology 128 (2009) e479–e486.
[47] N. Pozzi, E. Di Cera, Prothrombin structure: unanticipated features and opportunities 2014.
[48] B. Dahlbäck, Novel insights into the regulation of coagulation by factor V isoforms, tissue factor pathway inhibitorα, and protein S, J. Thromb. Haemost. 15 (2017) 1241–1250.
[49] E.A. Vogler, C.A. Siedlecki, Contact activation of blood-plasma coagulation, Biomaterials 30 (2009) 1857–1869.
[50] L. Suleiman, C. Négrier, H. Boukerche, Protein S: a multifunctional anticoagulant vitamin K-dependent protein at the crossroads of coagulation, inflammation, angiogenesis, and cancer, Crit. Rev. Oncol. Hematol. 88 (2013) 637–654.
[51] B. Furie, B.C. Furie, Mechanisms of thrombus formation, N. Engl. J. Med. 359 (2008) 938–949.
[52] A.L. Jones, M.D. Hulett, C.R. Parish, Histidine-rich glycoprotein: a novel adaptor protein in plasma that modulates the immune, vascular and coagulation systems, Immunol. Cell Biol. 83 (2005) 106–118.
[53] S. Wakabayashi, T. Koide, Histidine-rich glycoprotein: a possible modulator of coagulation and fibrinolysis, in: Semin. Thromb. Hemost., vol. 37, © Thieme Medical Publishers, 2011, pp. 389–394.
[54] N. Tsuchida-Straeten, S. Ensslen, C. Schäfer, M. Wöltje, B. Denecke, M. Moser, et al., Enhanced blood coagulation and fibrinolysis in mice lacking histidine-rich glycoprotein (HRG), J. Thromb. Haemost. 3 (2005) 865–872.
[55] S. Choudhary, P. Halbout, C. Alander, L. Raisz, C. Pilbeam, Strontium ranelate promotes osteoblastic differentiation and mineralization of murine bone marrow stromal cells: involvement of prostaglandins, J. Bone Miner. Res. 22 (2007) 1002–1010.
[56] V. Nardone, R. Zonefrati, C. Mavilia, C. Romagnoli, S. Ciuffi, S. Fabbri, et al., In vitro effects of strontium on proliferation and osteoinduction of human preadipocytes, Stem Cells Int. 2015 (2015) 1–12.
[57] Y. Kong, Y. Guo, J. Zhang, B. Zhao, J. Wang, Strontium promotes transforming growth factors β1 and β2 expression in rat chondrocytes cultured in vitro, Biol. Trace Elem. Res. 184 (2018) 450–455.
[58] U.M. Wewer, K. Ibaraki, P. Schjørring, M.E. Durkin, M.F. Young, R. Albrechtsen, A potential role for tetranectin in mineralization during osteogenesis, J. Cell Biol. 127 (1994) 1767–1775.
[59] I. Clemmensen, L.C. Petersen, C. Kluft, Purification and characterization of a novel, oligomeric, plasminogen kringle 4 binding protein from human plasma: tetranectin, Eur. J. Biochem. 156 (1986) 327–333.
[60] P. Gehron Robey, P. Bianco, J.D. Termine, The cellular biology and molecular biochemistry of bone formation, Disord. Bone Miner. Metab. (1992) 241–263.
[61] K. Iba, Y. Abe, T. Chikenji, K. Kanaya, H. Chiba, K. Sasaki, et al., Delayed fracture healing in tetranectin-deficient mice, J. Bone Miner. Metab. 31 (2013) 399–408.
[62] P. Dowling, C. Hayes, K.R. Ting, A. Hameed, J. Meiller, C. Mitsiades, et al., Identification of proteins found to be significantly altered when comparing the serum proteome from Multiple Myeloma patients with varying degrees of bone disease, BMC Genom. 15 (2014) 904.
[63] C. Thouverey, A. Malinowska, M. Balcerzak, A. Strzelecka-Kiliszek, R. Buchet, M. Dadlez, et al., Proteomic characterization of biogenesis and functions of matrix vesicles released from mineralizing human osteoblast-like cells, J. Proteom. 74 (2011) 1123–1134.
[64] B.M. Steiglitz, D.R. Keene, D.S. Greenspan, PCOLCE2 encodes a functional procollagen C-proteinase enhancer (PCPE2) that is a collagen-binding protein differing in distribution of expression and post-translational modification from the previously described PCPE1, J. Biol. Chem. 277 (2002) 49820–49830.